

## SdFFF monitoring of cellular apoptosis induction by diosgenin and different inducers in the human 1547 osteosarcoma cell line

C. Corbière<sup>a</sup>, S. Battu<sup>b,\*</sup>, B. Liagre<sup>a</sup>, P.J.P. Cardot<sup>b</sup>, J.L. Beneytout<sup>a</sup>

<sup>a</sup> *Laboratoire de Biochimie, Faculté de Pharmacie, EA 1085 "Biomolécules et Cibles Cellulaires Tumorales", Université de Limoges, 2 Rue du Dr. Marcland, 87025 Limoges Cedex, France*

<sup>b</sup> *Laboratoire de Chimie Analytique et Bromatologie, Faculté de Pharmacie, Université de Limoges, 2 Rue du Dr. Marcland, 87025 Limoges Cedex, France*

Received 10 February 2004; received in revised form 27 April 2004; accepted 17 May 2004

Available online 17 June 2004

### Abstract

Apoptosis is one of the most important phenomena of cellular biology. Sedimentation field flow fractionation (SdFFF) has been described as an effective tool for cell separation, respecting integrity and viability. Because SdFFF takes advantage of intrinsic properties of eluted cells (size, density, shape or rigidity), we investigated the capacity of SdFFF in monitoring the early and specific biophysical modifications which occurred during cellular apoptosis induction. Then, we used, as an *in vitro* cellular apoptosis model, the association between human 1547 osteosarcoma cells and diosgenin, a plant steroid known to induce apoptosis. Four other molecules were studied: hecogenin, tigogenin, staurosporine and MG132. Our results demonstrated a correlation between SdFFF elution profile changes (peak shape modification and retention ratio evolution) and effective apoptosis induction. For the first time, we demonstrated that SdFFF could be used to monitor apoptosis induction as early as 6 h incubation, suggesting different applications such as screening series of molecules to evaluate their ability to induce apoptosis, or sorting apoptotic cells to study apoptosis pathway.

© 2004 Elsevier B.V. All rights reserved.

**Keywords:** Sedimentation field flow fractionation; Apoptosis; Plant steroids; Diosgenin; Staurosporine; MG132

### 1. Introduction

Field Flow Fractionation (FFF) was conceptualized and developed in the late 1960s by Giddings [1]. This chromatographic-like separation family is described as one of the most versatile separation techniques [2–5]. The fundamental principle of FFF is based on the differential elution of species in a liquid (mobile phase) flowing through a ribbon-like capillary channel on a laminar mode [1–3]. FFF separation depends on specific particle susceptibility to an external field applied perpendicularly to the flat surface of the ribbon, and by consequence, perpendicularly to the flow direction [1–3]. Versatility of the FFF family is demonstrated by the wide range of external fields used which include gravitational, cross flow, electrical, magnetic or thermal fields, which define each FFF sub-family

[3,4]. While gravitational-FFF (GFFF) uses earth's gravity, the sedimentation-FFF (SdFFF), also called centrifugal- or multigravitational-FFF, uses a multigravitational external field generated by the rotation of the separation channel in a more complex device [2–5]. SdFFF appears to be particularly well suited for isolation and characterization of micron-sized species such as cells [3–6]. SdFFF elution mode for cells is described as "Hyperlayer" [3–5]. In such a mechanism, cell size, density, shape and rigidity are involved, as are channel geometry and flow rate characteristics. At constant flow rate and external field strength, larger, or less dense particles, are focused in faster streamlines and are eluted first [5–14]. As described [4,5,15,16], by taking advantage of intrinsic cell biophysical properties: size, density, rigidity or shape; SdFFF sorts viable cells which can be cultured for further use without specific labeling of any kind, in few minutes. Since the pioneering report of Caldwell et al. [6], which defined most of the basic rules and methodologies for cell separation, FFF, SdFFF and related technologies have shown a great potential for cell

\* Corresponding author. Tel.: +33 5 5543 5857; fax: +33 5 5543 5859.  
E-mail address: [battu@pharma.unilim.fr](mailto:battu@pharma.unilim.fr) (S. Battu).

separation and purification with major biomedical applications including hematology [11,17,18], cancer research [18–20], microorganism analysis [21–27], biochemistry and molecular biology [28–30]. More recently, we opened the field of neuroscience with the purification of neurons from a complex cell matrix [15], and provided sterile, usable and purified immature neural cell fractions without induction of cell differentiation [16].

Apoptosis, or programmed cell death, is a naturally occurring process of cell death that plays a fundamental role in the development of pluricellular organisms. Apoptosis maintains cellular homeostasis by replacing damaged or abnormal cells, with the aim to ensure tissue and organ functionalities and organism viability [31]. Factors that protect against apoptosis lead to prolonged survival of abnormal cells which favors the accumulation of genetic mutations and tumor promotion [32]. Apoptosis is characterized by several distinct morphological features and biochemical processes including cell shrinkage, plasma membrane blebbing, chromatin condensation, nucleosomal fragmentation and finally, formation of apoptotic bodies [33]. Over the last decade, many analytical tools have been developed to detect and characterize apoptotic cells such as molecular biology studies including p53 activation, caspase activities, increased Bax expression and DNA fragmentation [34,35].

Recently, Moalic et al. [34] described that diosgenin, a plant steroid, altered cell cycle and induced apoptosis in the human osteosarcoma 1547 cell line. In a second work [35], diosgenin was compared with two other plant steroids (hecogenin and tigogenin) in the same cell line and it was concluded that among these three plant steroids, diosgenin was the most effective in inducing cell death.

In this study, we investigated the capacity of SdFFF to be used for monitoring early and specific biophysical cell modifications which occurred during apoptosis. 1547 cells were treated with specific apoptotic inducers: diosgenin, staurosporine and MG132. Staurosporine is a protein kinase inhibitor and a strong inducer of apoptosis [36]. MG132 (carbobenzoxyl-leuciny-leuciny-norleucinal) is a highly potent proteasome inhibitor. It is well known that proteasome inhibition is associated with induction of cell death in actively proliferating cell lines [37]. Hecogenin and tigogenin, were also tested as less effective apoptosis inducers [35].

In this work, we demonstrated a direct correlation between effective molecular apoptosis induction and specific elution profile changes: retention ratio shift and peak shape modification. Our results also suggested that SdFFF is able to discriminate between effective apoptotic inducers depending on the mechanism of the apoptosis induction. Among techniques (light microscopy, Coulter Counter, ELISA) used to evaluate biophysical and biochemical changes occurring during 1547 cells apoptosis, only SdFFF elution appeared to be effective to take into account all the biophysical parameters involved: size, density, shape or rigidity.

For the first time, we demonstrated the effectiveness of using SdFFF as a simple and rapid method to monitor cellular apoptosis, as early as 6 h incubation. Many applications could be suggested such as the use of this model to screen series of molecules, or such as the use of SdFFF cell sorting ability to purify apoptotic populations to better understand apoptotic phenomena.

## 2. Theory

Two models of SdFFF elution modes are described for micron sized species such as cells: “Steric” and “Hyperlayer” [3,5–14]. In the “Hyperlayer” mode, the flow velocity/channel thickness balance generates a hydrodynamic lift force which drives the particles away from the accumulation wall. Species are then focused into a thin layer which corresponds to an equilibrium position in the channel thickness where the external field is exactly balanced by the hydrodynamic lift forces [3,5–14]. At this equilibrium position, the risk of cell-wall interactions is negligible, providing better cell separation. At equivalent density, large particles generate more lift forces and are focused in faster streamlines to be eluted first. The different average velocities of the different species are compared by means of the observed retention ratio  $R_{obs}$  which is the ratio of the void time versus the retention time  $= t_0/t_r$  [10]. Under the “Hyperlayer” elution mode, retention ratio  $R_{obs}$  is flow rate and external field dependent. At constant field, the increase in flow rate induces an increase in  $R_{obs}$ , and at constant flow the increase in field decreases  $R_{obs}$ . If the external field can be increased sufficiently, or flow rate decreased sufficiently to offset lift forces, micron-sized particles are confined into a very thin layer close to the accumulation wall. This elution mode is described as “Steric” [3,5–14] and appears as a limit case of “Hyperlayer”. By driving particles close to the accumulation wall, the “Steric” elution mode enhances cell/channel wall interactions which lead to channel poisoning with harmful consequences on cell integrity, viability and recovery [5,16].

Thus, SdFFF device setup and elution conditions were selected to promote the “Hyperlayer” elution mode against the “Steric” one [5].

## 3. Materials and methods

### 3.1. Cell line, cell culture and treatment

The 1547 human osteosarcoma cell line was kindly provided by Professor M. Rigaud (Laboratoire de Biochimie, Faculté de Médecine de Limoges, France). Freshly trypsinized cells were seeded at  $6 \times 10^5$  cells in 150 cm<sup>2</sup> tissue culture flasks, grown in Eagle’s minimum essential medium (Gibco BRL, Cergy-Pontoise, France) supplemented with 10% fetal calf serum (FCS) (Gibco BRL),

100 U/ml penicillin and 100 µg/ml streptomycin. Cultures were maintained in a humidified atmosphere with 5% CO<sub>2</sub> at 37 °C. Cells were allowed to adhere and grow for 3 days in culture medium prior to exposure to 40 µM diosgenin (Sigma, Saint Quentin-Fallavier, France), 40 µM hecogenin (Sigma), 40 µM tigogenin (Sigma), 0.1 µM staurosporine (Sigma) or 3 µM MG132 (Calbiochem, VWR International S.A.S. Pessac, France) for 6, 12 and 24 h. The same amount of vehicle was added to control cells. Adherent and floating cells were combined, counted and cell viability was determined by the trypan blue dye exclusion method. Cells were washed twice in phosphate-buffered saline (PBS pH 7.4) and cell concentration was adjusted to  $2 \times 10^6$  cells/mL before SdFFF analysis. For light microscopy, after 6 h treatment, cultured cells were fixed in phosphate-buffered saline (PBS) (pH 7.4) containing glutaraldehyde-formaldehyde (0.25–1%) for 2 min at 37 °C and washed in PBS, and observed by phase-contrast microscopy.

### 3.2. Apoptosis quantification

The 1547 cells were cultured in 6-well culture plates. After 40 µM diosgenin, 40 µM hecogenin, 40 µM tigogenin, 3 µM MG132 or 0.1 µM staurosporine treatment for 24 h, apoptosis was quantified by “cell death” enzyme-linked immunosorbent assay (ELISA) (Cell Death Detection ELISA<sup>PLUS</sup>, Roche Diagnostics, Meylan, France) on pooled fractions (adherent and floating cells). Cytosol extracts were obtained according to the manufacturer’s protocol and apoptosis was measured as previously described [34].

### 3.3. SdFFF device and cell elution conditions

The SdFFF separation device used in this study was derived from those previously described and schematized [15,16]. The separation channel was made up of two 870 mm × 30 mm × 2 mm polystyrene plates, separated by a Mylar<sup>®</sup> spacer in which the channel was carved. Channel dimensions were 785 mm × 10 mm × 0.125 mm with two V-shaped ends of 70 mm. The measured total void volumes (channel volume + connection tubing + injection and detection device) were  $960 \pm 5$  µL ( $n = 15$ ). Void volumes were calculated after injection and retention time determination of an unretained compound (0.1 g/L of benzoic acid, UV detection at 254 nm). Inlet and outlet 0.254 mm ID Peek<sup>®</sup> tubing (Upchurch Scientific, Oak Harbour, USA) were directly screwed to the accumulation wall. The channel-rotor axis distance was measured at  $r = 13.8$  cm. Sedimentation fields were expressed in units of gravity,  $1 g = 980 \text{ cm/s}^2$ , and calculated as previously described [15]. Two rotating seals were drilled to allow 0.254 mm ID Peek<sup>®</sup> tubing to fit in. A Water 590 HPLC programmable chromatographic pump (Waters Associates, Milford, MA, USA) was used to pump the sterile mobile phase. A M71B4 Carpanelli engine associated with a pilot unit Mininvert 370 (Richards Systems, Les Ullis, France), controlled the rotat-

ing speed of the centrifuge basket. Sample injections were done by means of a Rheodyne<sup>®</sup> 7125i chromatographic injection device (Rheodyne, Cotati, CA, USA). Cleaning and decontamination procedures, as well as devices involved in these processes, have been described in a previous report [5]. The elution signal was recorded at 254 nm by means of a Water 484 tunable absorbance detector (Waters Associates, Milford, MA, USA) and a 14-byte M1101 (100 mV input) acquisition device (Keithley Metrabyte, Tauton, MA, USA) operated at 2 Hz and connected to Macintosh computer. 1547 cell elution conditions were set up from 30 to 60 g as external field strength and from 0.4 to 1.0 mL/min as mobile phase flow rate. The optimal elution conditions (“Hyperlayer” mode) have been experimentally determined and were: flow injection through the accumulation wall of 100 µL 1547 cell suspension ( $2 \times 10^6$  cells/mL), flow rate: 0.6 mL/min, mobile phase: sterile PBS pH 7.4; external multi-gravitational field strength:  $40.00 \pm 0.03 g$ , spectrophotometer detection at  $\lambda = 254 \text{ nm}$ .

### 3.4. DAPI labeling

After 24 h treatment with 40 µM diosgenin, nuclear condensation was studied with DAPI (0.5 µg/ml) on 1547 cells before and after SdFFF analysis as described before [32]. For SdFFF, DAPI analysis was performed on cells specifically eluted in the 1547 cell peak (Fig. 1).

### 3.5. Coulter counter

A 256 channel Multisizer II Coulter Counter (Beckman Coulter, Fullerton, CA) was used to determine the mean cell population diameter. The cell suspension ( $2 \times 10^5$  cells) was diluted in Isoton<sup>®</sup> to a final volume of 15 mL. The counting conditions were: 500 µL sample volumes, cumulating three successive assays. Results are displayed as the mean  $\pm$  S.D. for three different experiments.

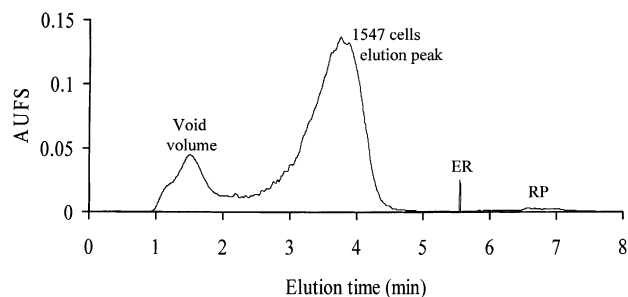


Fig. 1. Representative fractogram of 1547 osteosarcoma cells after SdFFF elution. Elution conditions: flow injection of 100 µL cell suspension ( $2 \times 10^6$  cells/mL), flow rate: 0.6 mL/min (sterile PBS pH 7.4); external multi-gravitational field:  $40.00 \pm 0.03 g$ , spectrophotometric detection at  $\lambda = 254 \text{ nm}$ . ER corresponds to the end of channel rotation, in this case the mean externally applied field strength was equal to zero gravity, thus RP, a residual signal, corresponds to the release peak of reversible cell-accumulation wall sticking.

### 3.6. Statistical analysis

The median and standard deviation (S.D.) were calculated using Excel software (Microsoft, Version 98). Statistical analysis of differences was carried out by analysis of variance (ANOVA test) using Statview (Version 5.0). A *P*-value of less than 0.05 (Fisher's PLSD test) was considered to indicate significance.

## 4. Results and discussion

Over the past decade, SdFFF and related technologies have demonstrated an important potential for cell sorting in major biomedical applications such as hematology, cancer research or molecular biology [18–20,28–30] or more recently, neurosciences [15,16]. During the same decade, apoptosis appeared as the one of the most studied phenomena in life sciences, and many analytical tools have been developed to detect and characterize the cellular apoptosis pathway [34,35].

In this work, in which SdFFF is not used as a cell sorter, we investigated for the first time, the SdFFF effectiveness in monitoring early and specific biophysical modifications (size, density, shape or rigidity) which occurred during cellular apoptosis induction. To achieve this goal, we selected the human 1547 osteosarcoma cell line/diosgenin association as an *in vitro* cellular apoptosis model. Four other molecules were studied: hecogenin, tigogenin, staurosporine and MG132.

### 4.1. SdFFF 1547 cell elution

When SdFFF is used for simple cell elution, as well as for cell sorting [5,15], many considerations must be taken into account such as (1) the respect of cell functional integrity; (2) providing a high level of cell viability without induction of apoptosis; and (3) providing high repeatability, reproducibility and recovery. To achieve these goals, specific SdFFF methodologies have been developed [5]. Thus, SdFFF elution conditions: flow injection of cell suspension, mobile phase flow rate: 0.6 mL/min; external field strength:  $40.00 \pm 0.03$  g, carrier phase composition (sterile isotonic buffer: PBS pH 7.4), polystyrene channel walls, as well as cleaning and decontamination procedures, are selected to promote the "Hyperlayer" elution mode and reduce particle-channel wall interactions [5].

Fig. 1 displays a representative elution fractogram obtained for control 1547 cells after 24 h culture. Two major peaks were observed: the first corresponded to unretained species (void volume peak:  $R_{\text{obs}} \approx 1$ ), and the second ( $R_{\text{obs}} = 0.421 \pm 0.007$ ,  $n = 15$ ) corresponded to the cell type. After total cell elution, the external field was stopped (ER, Fig. 1), and we can observe a residual signal (RP, Fig. 1) which corresponded to cell release from the separating channel. The absolute  $R_{\text{obs}}$  values depended on

the culture conditions and more precisely to the culture time.

In the "Hyperlayer" elution mode, micron-sized species show an  $R_{\text{obs}}$  that is flow rate and external field dependent. First, we measured the  $R_{\text{obs}}$  pattern of the specific cell peak for 3 days cultured 1547 cells (cultured cells prior incubation) under different elution conditions. At a constant field  $40.0 \pm 0.1$  g, the increase in flow rate induced an increase in  $R_{\text{obs}}$ :  $R_{\text{obs}} = 0.388 \pm 0.005$  at 0.4 mL/min and  $R_{\text{obs}} = 0.424 \pm 0.008$  at 1.0 mL/min (mean  $\pm$  S.D. for  $n = 3$ ). An increase of field at a constant flow rate (0.6 mL/min) decreased  $R_{\text{obs}}$  with  $R_{\text{obs}} = 0.444 \pm 0.006$  at 30.0 g and  $R_{\text{obs}} = 0.344 \pm 0.005$  at 60.0 g (mean  $\pm$  S.D. for  $n = 3$ ).

In the "Hyperlayer" mode, particles are driven away from the accumulation wall. Then, by using the following equation [12]:

$$R = \frac{6s}{\omega} \quad (1)$$

in which  $R$  is the retention ratio,  $\omega$  the channel thickness (125  $\mu\text{m}$ ),  $s$  the distance of the center of the focused zone from the channel wall [12], could be calculated. Using the  $R_{\text{obs}}$  value measured for 24 h control cells ( $0.421 \pm 0.008$ ,  $n = 15$ ), the average cell elevation  $s$  was 8.77  $\mu\text{m}$ . The mean diameter of 24 h control cells was  $14.20 \pm 0.35$   $\mu\text{m}$  ( $n = 3$ , Coulter Counter). Thus, the estimated cell radius ( $7.10 \pm 0.17$   $\mu\text{m}$ ) is less than the approximate average cell elevation value ( $s = 8.77$   $\mu\text{m}$ ). Finally, the effectiveness of this mode to reduce particle-accumulation wall interactions is shown in part by the low level of the corresponding cell release peak at the end of the fractogram (Fig. 1).

### 4.2. SdFFF monitoring of apoptotic cells

In this work, the association osteosarcoma 1547 cell line/diosgenin (plant steroid) is used as a model of cellular apoptosis induction *in vitro*. In this model, the mechanism and the biochemical pathway of apoptotic induction, which defined diosgenin effectiveness, have been described in previous reports [34,35]. Two other plant steroids were tested: hecogenin and tigogenin. In a recent report [35], we demonstrated that a minor difference in molecular structure between diosgenin and these two steroids (desaturation, addition of an hydroxyl group), led to a dramatic decrease in apoptosis induction compared to diosgenin [35]. These two molecules could be considered as weak apoptosis inducers. Finally, we also used two other well known apoptosis inducers in many cell lines: staurosporine and MG132 [38–44].

Before and after SdFFF elution, the percentage of cellular apoptosis was measured by nuclear DAPI staining, either in control or in treated 1547 cells. Our results show (Table 1), that SdFFF did not induce or modify the percentage of apoptosis.

It is well known that apoptosis is characterized by chromatin condensation and DNA fragmentation. In our study, quantitative determination of cytoplasmic histone-

Table 1

The percentage of cellular apoptosis was measured by nuclear DAPI staining, before and after SdFFF elution, either in control or in treated 1547 cells

	Before SdFFF elution	After SdFFF elution
Control 1547 cells	5.90 ± 1.30%	6.75 ± 1.25%
Diosgenin 40 µM (24 h)	19.77 ± 4.09%	23.00 ± 2.45%

Results are displayed as mean ± S.D. ( $n = 3$ ).

associated-DNA fragments (mono- and oligonucleosomes) was performed using ELISA after 24 h incubation. Results showed that DNA fragmentation was enhanced  $1.2 \pm 0.3$ -fold for hecogenin,  $2.7 \pm 0.3$ -fold for tigogenin,  $5.0 \pm 0.65$ -fold for diosgenin,  $32.4 \pm 2.2$ -fold for staurosporine and  $4.25 \pm 1.6$ -fold for MG132 compared to controls ( $n = 3$ ,  $P < 0.05$ ). Fig. 2 shows representative pictures of cell layers incubated for 6 h with the three major apoptosis inducers: diosgenin, staurosporine and MG132; for which we observed many morphological changes (Fig. 2), but no morphological changes were observed in cell cultures after 6 h incubation with tigogenin or hecogenin (data not shown).

Taken together, results of the ELISA apoptosis detection kit and cell culture observations demonstrated that, as previously described [34,35,38–44], diosgenin, staurosporine and

MG132 were effective apoptosis inducers, and that hecogenin and tigogenin were less effective.

Fractograms in Fig. 3 were representative of SdFFF elution of the different 1547 cell populations incubated in the absence (control cells) or in the presence of the three major apoptosis inducers, after 6, 12 or 24 h incubation. In all the cases, we observed a modification of the elution profile with a change in  $R_{\text{obs}}$  values: decreased with diosgenin, or an increased with staurosporine and MG132 (peak b, Fig. 3). Moreover,  $R_{\text{obs}}$  differences could be associated with peak shape modification such as the emergence of a new peak after MG132 incubation (Fig. 3, cases G and H, peak c). These changes were seen as early as 6 h incubation, while no significant cellular apoptosis could be measured by the ELISA apoptosis detection kit (data not shown). As SdFFF elution did not modify the percentage of apoptotic 1547 cells (Table 1), we concluded that these modifications (Fig. 3) were linked to specific cellular apoptosis induction, and were not due to non specific phenomena such as instrumental cell destruction or trapping. Concerning hecogenin and tigogenin, only small changes in the elution profiles were observed after 24 h incubation for tigogenin (Fig. 4), a more efficient apoptosis inducer than hecogenin [35].

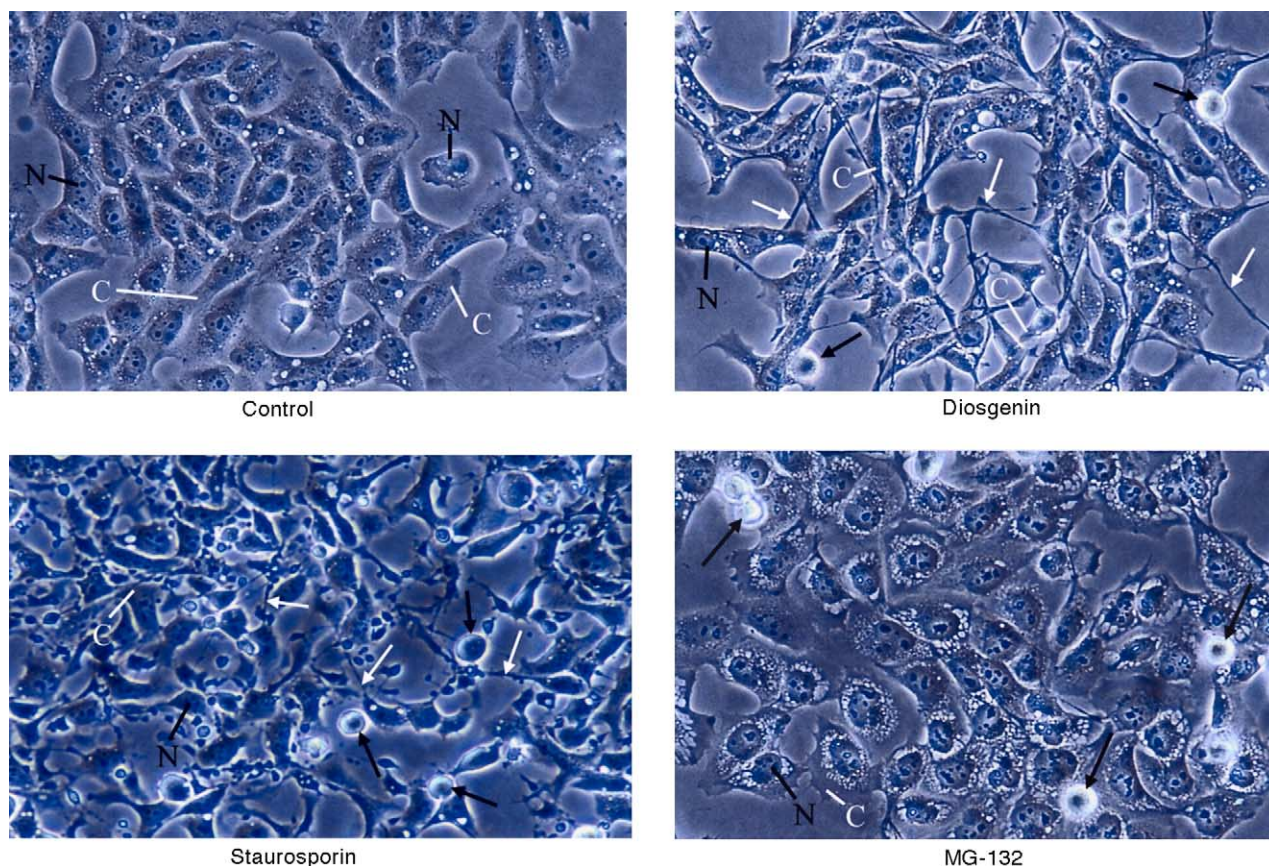


Fig. 2. Cellular morphological modifications. Microscopic observations of 1547 cell culture incubated for 6 h in the absence (control) or in the presence of 40 µM diosgenin, 0.1 µM staurosporine or 3 µM MG132 (magnification 400×). Cytoplasm condensation (black arrows); cytoplasmic filaments (white arrows); N = nucleus; C = cytoplasm.

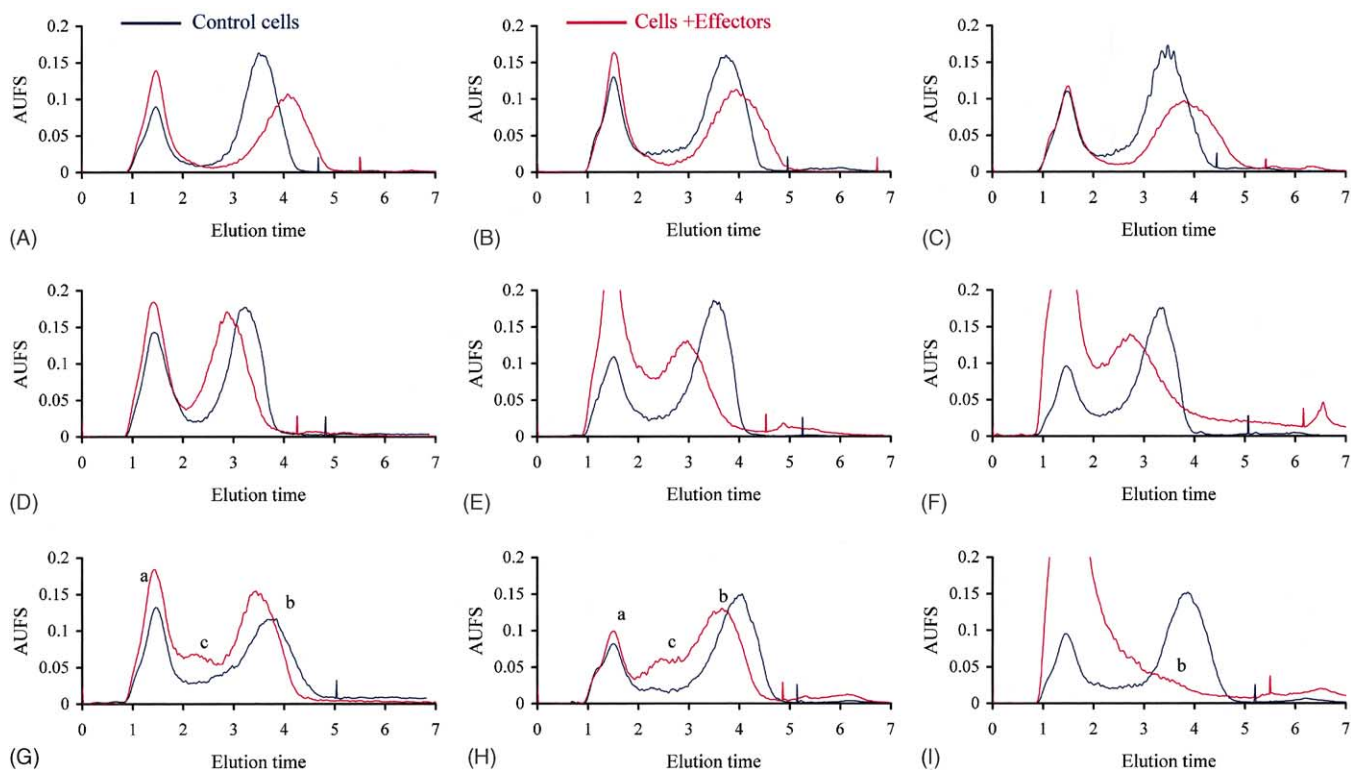


Fig. 3. Elution profiles obtained during apoptosis. Representative fractograms of 1547 osteosarcoma cells incubated for 6, 12 or 24 h in the absence (control) or in the presence of 40  $\mu\text{M}$  diosgenin, 0.1  $\mu\text{M}$  staurosporine or 3  $\mu\text{M}$  MG132 (effectors). Elution conditions: flow injection of 100  $\mu\text{L}$  cell suspension ( $2 \times 10^6$  cells/mL), flow rate: 0.6 mL/min (sterile PBS pH 7.4); external multi-gravitational field:  $40.00 \pm 0.03$  g, spectrophotometric detection at  $\lambda = 254$  nm. A, B and C: diosgenin for 6, 12 and 24 h incubation, respectively. D, E and F: staurosporine for 6, 12 and 24 h incubation, respectively. G, H and I: MG132 for 6, 12 and 24 h incubation, respectively; a corresponds to the void volume peak, b corresponds to the 1547 cell elution peak and c corresponds to the new peak.

Thus, as no complex sample preparation is needed, SdFFF appeared to be a good method to quickly evaluate and discriminate (less than 10 min) between apoptotic potentials for different molecules by the observation of elution profile modifications in comparison to control populations.

The measurement of  $R_{\text{obs}}$  changes could be used to monitor global apoptosis evolution in a cell population, but, we also observed  $R_{\text{obs}}$  shifts and peak shape modifications depending on the inducer used (Fig. 3). For example, dios-

genin led to a decrease in  $R_{\text{obs}}$ , while MG132, which induced apoptosis to the same extent (ELISA detection kit), led to the appearance of a new population with an increase in  $R_{\text{obs}}$  values (Fig. 3A–C versus G–I). Thus, results displayed in Fig. 3 suggested that diosgenin, staurosporine or MG132 did not modify the intrinsic biophysical cell properties in the same manner.

We demonstrated, in the first part of this study, that 1547 cells were eluted under the “Hyperlayer” mode. As described

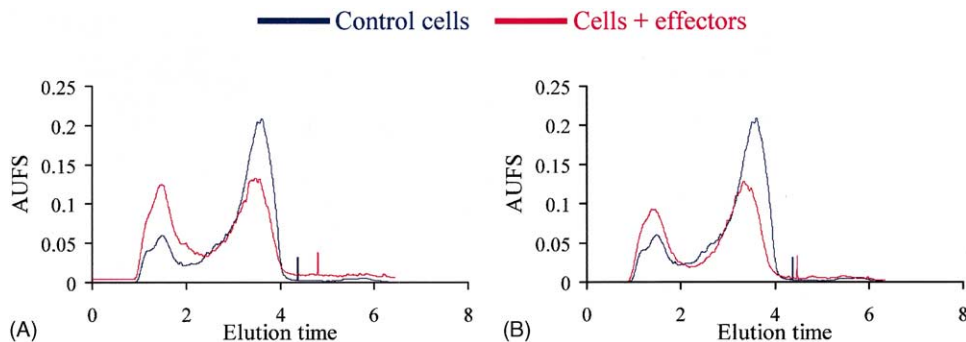


Fig. 4. Elution profiles evolution during apoptosis. Representative fractogram of 1547 osteosarcoma cells incubated for 24 h in the absence (control) or in the presence of 40  $\mu\text{M}$  hecogenin or 40  $\mu\text{M}$  tigogenin (effectors). Elution conditions: flow injection of 100  $\mu\text{L}$  cell suspension ( $2 \times 10^6$  cells/mL), flow rate: 0.6 mL/min (sterile PBS pH 7.4); external multi-gravitational field:  $40.00 \pm 0.03$  g, spectrophotometric detection at  $\lambda = 254$  nm; A: hecogenin, B: tigogenin.

before [3,5–14], at equivalent densities, the “Hyperlayer” elution mode predict a size dependant cell elution order: large cells are eluted first; and at equivalent size, a density dependant cell elution order: denser cells are eluted last. Moreover, cell shape and rigidity influence the cell elution order [11].

In order to verify the impact of cell size changes on SdFFF profile modifications, and therefore the impact of density modification, we measured the mean cell diameter by Coulter Counter. The difference between the mean cell diameter (Fig. 3) after incubation in the presence of apoptosis inducers minus the mean control cell diameter was, after 6 and 24 h incubation: 0.53 and 1.37  $\mu\text{m}$  for diosgenin 40  $\mu\text{M}$ , 1.04 and 1.80  $\mu\text{m}$  for MG132 3  $\mu\text{M}$ , 0.33 and 2.15  $\mu\text{m}$  for staurosporine 0.1  $\mu\text{M}$ . It is shown, that, whatever the inducer studied (diosgenin, staurosporine or MG132) or incubation time, we observed an increase in cell diameter. For staurosporine and MG132, results were in agreement with a size dependent elution order for “Hyperlayer” for which the increase in cell size is correlated with an increase in  $R_{\text{obs}}$ , assuming no modifications of cell density.

Fig. 5 shows the particle size distribution (PSD) obtained by Coulter Counter for control and 1547 cells incubated for 12 h with MG132. These results confirm that the shift of peak b in Fig. 3 (Fig. 3, cases G and H), is due to a size increase. However, the Coulter Counter results do not show a size population that corresponds with peak c (Fig. 3, cases G–I).

SdFFF retention is based on size and density, and in the absence of a size difference, diosgenin results suggest an increase in density [3,5–14]. The size and PSD results obtained using Coulter Counter are not sufficient to explain SdFFF profile evolutions and to monitor apoptosis induction.

If mean size and PSD modification are easy to determine using a Coulter Counter, the role of cell density, shape or rigidity are more difficult to discriminate. Nevertheless, the SdFFF elution profile modification suggested either a major change in the size/density balance with a first order influ-

ence, or a complex, with second order influence, of cell rigidity or shape. For example, as shown in Fig. 2, we observed that three different apoptotic inducers led to important but different morphological changes after 6 h incubation.

Our results showed a direct correlation between SdFFF elution profile modifications and cell apoptosis induction *in vitro*. Among techniques used to evaluate the biophysical and biochemical changes in apoptotic 1547 cells: DAPI staining, light microscopy, Coulter Counter, ELISA cell death detection kit; SdFFF appeared as an effective tool to study apoptosis by taking into account the major biophysical parameter changes occurring during apoptosis induction. By comparison with classical techniques used to shown apoptosis induction in the 1547 cell line: DAPI staining, light microscopy, and ELISA detection kit; we demonstrated that SdFFF could be used at a very early stage of apoptosis induction when microscopy was not specific or when DAPI or ELISA tests are insufficiently sensitive. The other advantages for using SdFFF are that (1) SdFFF is a simple technique (no complex mobile phase and no long or expensive cell preparation); (2) SdFFF is faster in comparison to other techniques (fractionation in less than 10 min); and (3) that the device is easily and quickly setup for each new separation problem.

Thus, after acquisition of a reference profile, SdFFF alone, as early as 6 h incubation, could be used to monitor and screen cell apoptosis induction by series of molecules.

Finally, as previously described [4,5,15,16], SdFFF sorts, in few minutes, viable, sterile and usable cells which can be cultured for further applications without specific labeling of any kind. Thus, we can suggest using in a future work, SdFFF cell sorting to purify apoptotic cells, in particular the new cell population observed after MG132 incubation, in order to better understand and identify the biochemical processes of apoptosis.

## 5. Conclusion

Taken together, our results demonstrated a direct correlation between SdFFF elution profile modifications (retention ratio shift, emergence of a new peak) and cellular apoptosis induction *in vitro*.

As SdFFF takes advantage of intrinsic biophysical properties of eluted cells, it appeared to be a good tool to study many life-science domains because (1) no complex mobile phase and no long, expensive cell preparation or labeling are needed; (2) elution is fast; and (3) the device is easily and quickly setup for each new separation problem. Thus, in comparison to other methods used to follow apoptosis, SdFFF performed under strictly defined conditions (“Hyperlayer” elution mode), is a rapid, simple and useful device to monitor complex apoptosis induction, as early as 6 h incubation.

These results also suggested different applications such as screening the *in vitro* apoptotic potential for series of

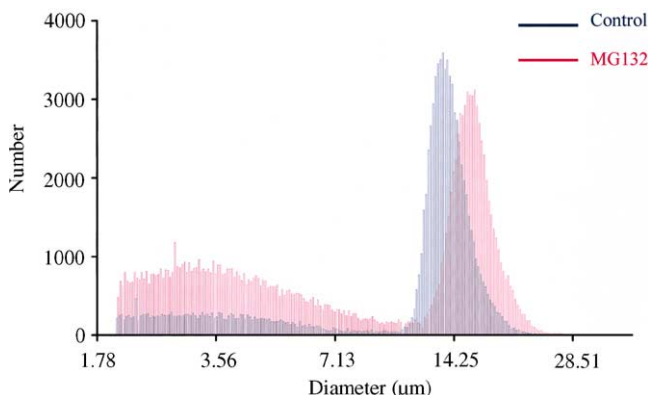


Fig. 5. Comparison of representative particle size distribution profiles. Particle size distribution profiles were performed by using Coulter Counter on 1547 osteosarcoma cells incubated for 12 h in the absence (control) or in the presence of 3  $\mu\text{M}$  MG132.

molecules, or sorting apoptotic cells in order to study complex apoptotic phenomenon.

## Acknowledgements

We are grateful to Professor M. Rigaud (Laboratoire de Biochimie Médicale, Faculté de Médecine, Limoges, France) for providing the 1547 human osteosarcoma cell line. We would like to thank Dr. J. Cook-Moreau and D. Léger for technical assistance and helpful discussions in the preparation of this manuscript. The expenses of this work were defrayed in part by the Ministère de l'Éducation Nationale, de la Recherche et de la Technologie, the Conseil Régional du Limousin and by the Fond Social Européen.

## References

- [1] J.C. Giddings, *Sep. Sci.* 1 (1966) 123.
- [2] M.N. Myers, *J. Microcolumn Sep.* 9 (1997) 151.
- [3] J.C. Giddings, in: M.E. Schimpf, K. Caldwell, J.C. Giddings (Eds.), *Field-Flow Fractionation Handbook*, Wiley, New York, 2000, p. 3.
- [4] T. Chianea, N.E. Assidjo, P.J.P. Cardot, *Talanta* 51 (2000) 835.
- [5] S. Battu, J. Cook-Moreau, P.J.P. Cardot, *J. Liq. Chromatogr. Relat. Technol.* 25 (2002) 2193.
- [6] K.D. Caldwell, Z.Q. Cheng, P. Hradecky, J.C. Giddings, *Cell Biophys.* 6 (1984) 233.
- [7] K.D. Caldwell, T.T. Nguyen, T.M. Murray, M.N. Myers, J.C. Giddings, *Sep. Sci. Technol.* 14 (1979) 935.
- [8] M.R. Schure, K.D. Caldwell, J.C. Giddings, *Anal. Chem.* 58 (1986) 1509.
- [9] M. Martin, P.S. Williams, in: F. Dondi, G. Guiochon (Eds.), *Theoretical Advancement in Chromatography and Related Separation Techniques*, Kluwer, Dordrecht, 1992, p. 513.
- [10] P.S. Williams, S. Lee, J.C. Giddings, *Chem. Eng. Commun.* 130 (1994) 143.
- [11] X. Tong, K.D. Caldwell, *J. Chromatogr. B* 674 (1995) 39.
- [12] J. Chmelik, *J. Chromatogr. A* 845 (1999) 285.
- [13] K.D. Caldwell, in: M.E. Schimpf, K.D. Caldwell, J.C. Giddings (Eds.), *Field-flow Fractionation Handbook*, Wiley, New York, 2000, p. 79.
- [14] J. Plockova, F. Matulik, J. Chmelik, *J. Chromatogr. A* 955 (2002) 95.
- [15] S. Battu, W. Elyaman, J. Hugon, P.J.P. Cardot, *Biochim. Biophys. Acta* 1528 (2001) 89.
- [16] C. Lautrette, P.J.P. Cardot, C. Vermot-desroche, J. Wijdenes, M.O. Jauberteau, S. Battu, *J. Chromatogr. B* 791 (2003) 149.
- [17] E. Urbankova, A. Vacek, J. Chmelik, *J. Chromatogr. B* 687 (1996) 449.
- [18] X.B. Wang, J. Yang, Y. Huang, J. Vykoukal, F.F. Becker, P.R. Gascoyne, *Anal. Chem.* 72 (2000) 832.
- [19] J. Yang, Y. Huang, X.-B. Wang, F.F. Becker, P.R.C. Gascoyne, *Anal. Chem.* 71 (1999) 911.
- [20] Y. Huang, J. Yang, X.B. Wang, F.F. Becker, P.R. Gascoyne, *J. Hematho. Stem Cell* 8 (1999) 481.
- [21] P. Gascoyne, C. Mahidol, M. Ruchirawat, J. Satayavivad, P. Watcharasit, F.F. Becker, *Lab Chip* 2 (2002) 70.
- [22] P. Reschiglian, A. Zattoni, B. Roda, L. Cinque, D. Melucci, R. Min Byung, H. Moon Myeong, *J. Chromatogr. A* 985 (2003) 519.
- [23] P. Reschiglian, A. Zattoni, B. Roda, S. Casolari, M.H. Moon, J. Lee, J. Jung, K. Rodmalm, G. Cenacchi, *Anal. Chem.* 74 (2002) 4895.
- [24] R. Sanz, P. Cardot, S. Battu, M.T. Galceran, *Anal. Chem.* 74 (2002) 4496.
- [25] R. Sanz, B. Torsello, P. Reschiglian, L. Puignou, M.T. Galceran, *J. Chromatogr. A* 966 (2002) 135.
- [26] S. Saenton, H. Lee, Y.-S. Gao, J.F. Ranville, S.K.R. Williams, *Sep. Sci. Technol.* 35 (2000) 1761.
- [27] A. Khoshmanesh, R. Sharma, R. Beckett, *J. Environ. Eng.-ASCE* 127 (2001) 19.
- [28] M. Nilsson, P.T. Kallio, J.E. Bailey, L. Buelow, K.-G. Wahlund, *Biotechnol. Prog.* 15 (1999) 158.
- [29] H. Lee, S.K.R. Williams, S.D. Allison, T.J. Anchordoquy, *Anal. Chem.* 73 (2001) 837.
- [30] I. Park, K.-J. Paeng, Y. Yoon, J.-H. Song, M.H. Moon, *J. Chromatogr. B* 780 (2002) 415.
- [31] R. Duval, S. Delebassée, P.J.P. Cardot, C. Bosgiraud, *Arch. Virol.* 147 (2002) 943.
- [32] S. Battu, M. Rigaud, J.L. Beneytout, *Anticancer Res.* 18 (1998) 3579.
- [33] A.H. Wyllie, *Br. Med. Bull.* 53 (1997) 451.
- [34] S. Moalic, B. Liagre, C. Corbière, A. Bianchi, M. Dauca, K. Bordji, J.L. Beneytout, *FEBS Lett.* 506 (2001) 225.
- [35] C. Corbière, B. Liagre, A. Bianchi, K. Bordji, M. Dauca, P. Netter, J.-L. Beneytout, *Int. J. Oncol.* 22 (2003) 899.
- [36] T. Tamaoki, H. Nomoto, I. Takahashi, Y. Kato, M. Morimoto, F. Tomita, *Biochem. Biophys. Res. Commun.* 135 (1986) 397.
- [37] H.C. Drexler, *Proc. Natl. Acad. Sci. U.S.A.* 94 (1997) 855.
- [38] U.G. Lopes, P. Erhardt, R. Yao, G.M. Cooper, *J. Biol. Chem.* 272 (1997) 12893.
- [39] X.M. Fan, B.C. Wong, W.P. Wang, X.M. Zhou, C.H. Cho, S.T. Yuen, S.Y. Leung, M.C. Lin, H.F. Kung, S.K. Lam, *Int. J. Cancer* 93 (2001) 481.
- [40] B. Wagenknecht, M. Hermisson, K. Eitel, M. Weller, *Cell. Physiol. Biochem.* 9 (1999) 117.
- [41] B. Wagenknecht, M. Hermisson, P. Groscurth, P. Liston, P.H. Kramer, M. Weller, *J. Neurochem.* 75 (2000) 2288.
- [42] Y.T. Hsu, K.G. Wolter, R.J. Youle, *Proc. Natl. Acad. Sci. U.S.A.* 94 (1997) 3668.
- [43] D. Tang, J.M. Lahti, V.J. Kidd, *J. Biol. Chem.* 275 (2000) 9303.
- [44] I. Jeremias, I. Herr, T. Boehler, K.M. Debatin, *Eur. J. Immunol.* 28 (1998) 143.